

MIC2015 – 15th Machining Innovations Conference for Aerospace Industry  
**Simulation and evaluation of different process strategies in a 5-axis re-contouring process**

Berend Denkena<sup>a</sup>, Volker Böß<sup>a</sup>, Dennis Nespor<sup>a,\*</sup>, Felix Rust<sup>a</sup>

<sup>a</sup>*Institute of production engineering and machine tools (IFW), An der Universität 2, Garbsen 30823*

\* Corresponding author. Tel.: +49-511-7624299; fax: +49-511-7625115. E-mail address: nespor@ifw.uni-hannover.de

**Abstract**

In the regeneration of turbine or compressor blades each blade damage is varying in location, size and shape, depending on the cause of damage. An important regeneration step is the re-contouring which is applied after the deposit welding to remove excess material. With complex blade shapes this step requires 5-axis machining methods. Due to different cases of damage, the re-contouring has to be adapted to each individual repair case to satisfy the high quality requirements regarding the final workpiece. This paper combines the two topics machining strategy and emerging workpiece quality. In this context the work demonstrates a simulation-based approach for the 5-axis re-contouring process. Hence, different 5-axis tool-paths strategies are applied on an analogy repair case including a modelled weld shape. The re-contouring is performed virtually via a dixel based material removal simulation as well as experimentally by using a 5-axis milling machine. Afterwards an evaluation of the different tool-path strategies is done considering achieved workpiece quality. The results imply that the simulation is applicable to predict certain aspects of the workpiece quality such as surface topography. With the simulation system, a tool-path evaluation is possible before re-contouring real workpieces.

© 2015 The Authors. Published by Elsevier B.V. This is an open access article under the CC BY-NC-ND license

(<http://creativecommons.org/licenses/by-nc-nd/4.0/>).

Peer-review under responsibility of the International Scientific Committee of the “New Production Technologies in Aerospace Industry” conference

**Keywords:** milling; simulation; re-contouring; blade repair

**1. Introduction**

*1.1. Regeneration and re-contouring*

The repair of expensive goods like blades and vanes of aircraft engine components is daily practice in Maintenance, Repair and Overhaul (MRO) business. However, the process chain significantly differs from part to part. The repair process consists of pre-inspection, material deposit, re-contouring and a post-inspection, see figure 1 [1].

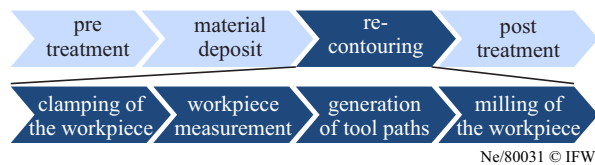


Fig. 1. Process chain of regeneration and re-contouring

The re-contouring, which is the final shape cutting of the blade, has a major influence on the performance of the repaired

blade. A high accuracy in surface finish is important for compliance with performance and safety regulations for the aircraft engine. One challenge for the MRO industry arises from the reverse engineering of the repair part with unknown material deposit plus the deviated shape of the part. This has been addressed by various researchers [2–4]. Though the re-contouring process is daily practice in industry, it has not been intensively examined from a scientific base. Nowadays, re-contouring mostly falls back on adjustment of a predefined tool path based on position identification of the workpiece and an adaption of the tool path offset. Scientific based researches use offset-based tool-paths as well, to provide reliability and repeatability in process, as seen in figure 2.

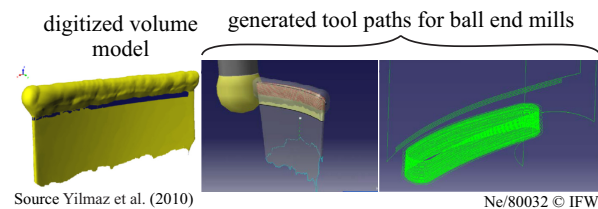


Fig. 2. Tool path strategy for tip repair used by Yilmaz et al. [3]

Companies have established, offering specialized software to adapt tool-paths for the re-contouring of blades and vanes, e.g. TTL or BCT [5,6]. For this purpose a Master CAD model of the blade is fitted to the individual shape of each blade. Nevertheless, tool path adaption in these cases does not consider the deposit material and the changing tool engagement conditions. The process development and run-in processes on the machine tools based on experience. This can lead to form deviation, undetermined part properties and even scrap parts [7,8]. From a scientific point of view, it has been pointed out that the shape of the deposit material respective the weld is of major importance regarding the re-contouring step. This has been shown through experiments and simulations on the titanium alloy Ti-6Al-4V [9]. An active guiding system has been established to compensate tool deflections while re-contouring [10]. Blade digitization is applied by reverse engineering of the blade, which leads to suitable CAD data for further processing [3,4]. To provide a proper clamping of the workpiece, different clamping methods were examined. Pin-type clamping has been found to be a solution for the demands of differing blade roots [11,12]. These works show the potential and the possibilities for adaptive machine functions. However, the tool-path itself has not been explicitly considered. Assuming the shape of the deposit material is known from blade digitization, a material removal simulation can be used to reach a higher adaptability of the tool-path. The simulation therefore serves for examining dimensional accuracy and furthermore for prognosis of forces and residual stresses. Hence, the scientific view on tool-path planning and re-contouring technology cannot be separated from each other.

### 1.2. Simulation approaches for manufacturing of parts

In the last decades enormous effort has been put into prediction of certain aspects of the machining process, e. g. cutting forces, surface quality or residual stresses. These three aspects are described in the following because of their high importance for re-contouring high value parts. The prediction of cutting forces is one subject of research for almost 100 years. All methods can be classified into analytical, empirical and numerical models or combined, so called hybrid approaches [13–17]. One of the most established methods are the mechanistic models, which use empirical, material-specific cutting force coefficients, combining them with process specific undeformed chip dimensions such as uncut chip thickness. This type of cutting forces models can also be enhanced with additional terms in order to consider e.g. the indentation effect due to low cutting speeds at the tool tip for ball end milling processes [17]. It is shown, that mechanistic models are also applicable for re-contouring due to the low influence of the weld inhomogeneity [9].

The surface topography is often predicted by modelling the cutting edge kinematics by numerical or analytical methods [18–20]. The universal, numerical approach is the usage of a material removal simulation using e.g. dixel, voxel or constructive solid geometries (CSG) for workpiece definition [21]. Besides surface topography prediction, the material removal simulations are also used for cutting force prediction [9,22]. It has to be mentioned that the influence of tool micro-geometry is less investigated than the influences of specific process kinematics for surface topography simulations.

The cause-effect relationships of residual stress formation

after machining is still not fully understood as shown by Jawahir et al. [23]. One possible reason is the high interaction between the most influencing factors to residual stresses, which are the choice of the material, the machining process and the tool micro-geometry. Most residual stress predictions are based on FE-Simulations [24] or hybrid methods [25]. The prediction methods in literature aim to virtualize the machining process to reduce or eliminate physical trails to ensure the workpiece quality or improving performance [26]. This is also important for the re-contouring process but these methods are not applied for 5-axis machining yet. Virtual machining processes use tool-workpiece-engagement algorithms. For the work described in this paper, a multi dixel model was used in order to verify different re-contouring strategies. The first part describes an analog workpiece providing a realistic interference contour, which is re-contoured on a 5-axis machine tool. Three derived tool-path strategies are applied afterwards for the re-contouring of the workpiece. Further on, the tool path strategies are considered in simulation and experiments. The measured factors of workpiece quality, namely surface topography and residual stresses are compared to the simulation results. Also it is shown in simulation, how process forces vary between each process strategy.

## 2. Manufacturing of the analog workpieces

Due to the individual material deposit each workpiece differs in re-contouring applications. Different workpieces would change the initial situation for comparing different tool path strategies and to verify the methods for prediction. Therefore an analog workpiece is milled from a whole piece which emulates a repaired blade. This method is valid, because the influence of the inhomogeneity of the weld is negligible [9]. The thickness of the analog workpieces is increased in order to reduce the influence of workpiece vibrations during re-contouring and to ensure the transferability of previous findings. Another advantage of the analog workpieces is that the re-contouring can be applied in the same clamping as the manufacturing. This eliminates the inaccuracies of the workpiece measurements, which is an issue in practice. Two different repair methods are included at the analog workpiece. The first is the patch repair, where the damaged part of the blade is removed and replaced by a spare part, called patch [27]. The second is the established tip-repair, which is used to decrease the gap between the blade and the case. Figure 3 shows the CAD-model and the corresponding workpiece after 5-axis machining, which are virtually re-contoured by three different strategies. Due to its more complex shape, only the weld is considered for further progression in re-contouring.

## 3. Simulation methods for re-contouring

The virtualization of the re-contouring process is utilized with the material removal simulation CutS [28], which uses a dixel model for workpiece discretization. The simulation environment considers the real tool geometry and the tool kinematic instead of a body of rotation, which is a sphere in the case of ball end mills. The advantage of the consideration of the cutting edge movement by angular steps is more realistic surface

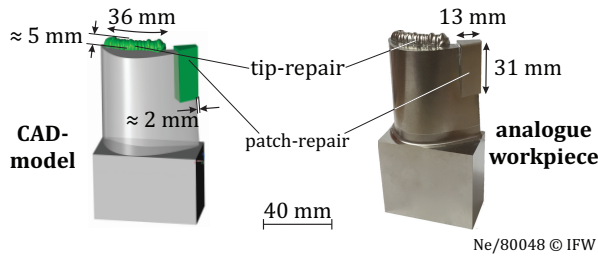


Fig. 3. Comparison between CAD-Model and final analog workpiece

topography, but the disadvantage is the low simulation speed compared due to the use of the original cutter contour.

### 3.1. Process forces

The simulation of the cutting process is divided to small time steps which results in angular steps due to the rotation of the tool. During the time period of an angular step  $\Delta\varphi$  a certain volume is removed. This volume is approximated through a so called swept volume. In [9] an algorithm is presented to convert the swept volume into uncut chip thickness  $h$ , engaged cutting edge length  $S$  etc. for forces prediction. This algorithm is improved and extended for this research. The first step of the algorithm is a discretization of the swept volume into planes and calculating the intersections of all dixel in X-, Y-, and Z-direction. The extension to a multi-dixel environment was necessary in order to increase precision for 5-axis strategies as shown in figure 4. It has been shown that the most important aspect for cutting forces prediction is the density of the removed dixel inside the swept volume. Low dixel density leads to numerical noise of the uncut chip thickness and thus to low quality of cutting force prediction.

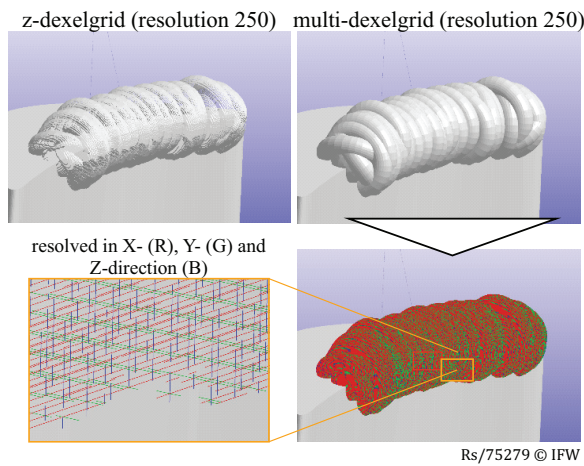
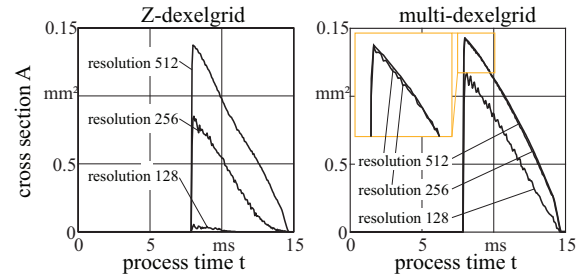


Fig. 4. Multi-dixel simulation environment

This interdependency is shown in figure 5 comparing the evaluated cross section  $A$  using a Z-dixelgrid and a multi-dixelgrid. It can be seen, that the multi-dixelgrid provides a higher dixel density, which leads to a reduction of numerical noise and more accurate results. The positive effect of a multi-dixel grid becomes significant, if high inclination angles are

applied. This is due to the discretization of the swept volume along the tool axis, as presented in [9]. The angle step  $\Delta\varphi$ , which is the trochoidal cutting edge movement due to time discretization of the simulation, has a lower influence on the prediction of the cutting forces.



### slot milling with ball end mill (simulation)

cutting speed  $v_c = 40$  m/min lead angle  $\lambda = 60^\circ$   
 feed per tooth  $f_z = 0.2$  mm tilt angle  $\tau = 60^\circ$   
 depth of cut  $a_p = 0.5$  mm workpiece: 4x4x2 mm  
 Ne/81805 © IFW

Fig. 5. Influence of dixel density on the cross section  $A = bh$

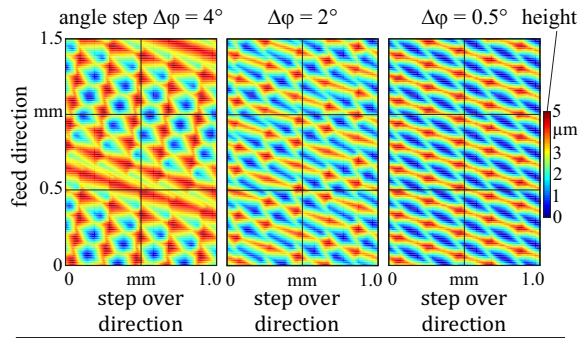
### 3.2. Surface topography

The final topography of the blade is influenced by a variety of parameters. These are e.g. tool shape, cutting edge errors, tool- and workpiece deflections as well as material properties and clamping errors. Nevertheless, this work considers a rotating tool providing the original shape of the edge. Errors regarding tool or workpiece clamping are not considered. Thus the kinematic topography is simulated based on the tool path strategies. The tool deflection is calculated based on process forces using a linear cantilever model. This is valid for most applications [29] by including the influence of the tool holder and the machine tool. The stiffness results from the force/displacement ratio.

In contrast to the simulation of process forces, the simulated surface topography is highly influenced by the angle step of tool rotation. The angle step  $\Delta\varphi$  for the time step  $\Delta t$  is calculated as follows

$$\Delta\varphi = \frac{n \cdot 360^\circ}{60 \cdot \Delta t} \quad (1)$$

Where  $n$  is the rotational speed of the tool. Therefore the time discretization  $\Delta t$  has to be adjusted for different cutting speeds to keep the angle step  $\Delta\varphi$  constant. Figure 6 shows the changing surface topographies for an angle step between  $0.5^\circ$  and  $4^\circ$ . It can be seen, that a high angle step results in an inaccurate computed surface including simulation defects. By decreasing the angle step  $\Delta\varphi$ , the accuracy of the surface is improved, but the simulation speed is decreased. In this case an angle step of  $\Delta\varphi = 0.5^\circ$  is chosen due to its good compromise between simulation speed and accuracy. Simulated topography with angle step of  $\Delta\varphi = 0.25^\circ$  and below show no differences to the topography simulated with  $\Delta\varphi = 0.5^\circ$ .



#### surface topography simulation with ball end mill

cutting speed  $v_c = 40$  m/min    depth of cut  $a_p = 0.4$  mm  
 feed per tooth  $f_z = 0.15$  mm    step over  $b_r = 0.2$  mm  
 lead angle  $\lambda = 60^\circ$     tilt angle  $\tau = 60^\circ$

Ne/80043 © IFW

Fig. 6. Influence of rotation increment on kinematic surface topography

### 3.3. Surface topography

The prediction of residual stresses is still a major task in science [23]. Whereas the residual stresses after orthogonal turning processes are often successfully simulated by FEM [30,31], more complex processes like milling or cylindrical turning often use hybrid approaches to consider specific aspects of the cutting process [25,32]. Therefore, in this work a hybrid model approach is applied by using a material specific empirical coefficient  $K$  and the ploughing forces  $F_{pl}$  for the case of ball end milling of Ti64. This approach only considers the cross section of the milling process, which is in contact to the final surface. This concept was introduced by Denkena et al. [33] and is visualized in figure 7. The forces of the green area are called surface generating forces and are considered in the following. Using the force model of [15] and only using the term with the edge-coefficients, leads to a good representation of the ploughing effect. Furthermore, these forces are related to an area, called  $A_{sp}$ , which is the area of the final generated surface during the angular step  $\Delta\varphi$ . The surface generating ploughing forces and the area  $A_{sp}$  are applied to

$$S \sim \log(F_{pl}) \cdot \sqrt{A_{sp}} \quad (2)$$

It has to be mentioned that this approach is not for simulation of the residual stress, but the parameter  $S$  is reasonable to describe the influence of the ball end milling process to the final residual stress state in the workpiece. More details about this approach are described in [33].

## 4. Experiments and Simulations

### 4.1. Re-contouring strategies

Three different re-contouring strategies with different tool paths are considered in this paper. Even though different tool paths are used for re-contouring, the final surface is generated

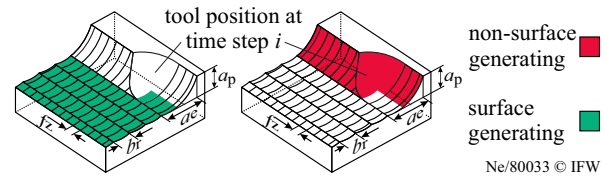


Fig. 7. Principle of surface generation using ball end mills

by a ball end mill (SECO, type JH970100,  $D = 10$  mm,  $z = 2$ ) using the same feed per tooth  $f_z$  and step over  $b_r$  for all three strategies. The first re-contouring strategy is the simplest one and comparable to established tool paths in industry as described in section 1.1. In this case, the shape of the weld is not considered by the strategy and the tool path is adapted to undamaged parts of the workpiece. This leads to a maximum and varying depth of cut  $a_p$  due to the shape of the weld and to maximal cutting forces compared to the other two strategies. The final surface is generated by the first cut without roughing and without sequential tool paths. The tool path of strategy 1 is schematically pictured in figure 8. Nevertheless, this strategy is the fastest with a process time of 12 min.

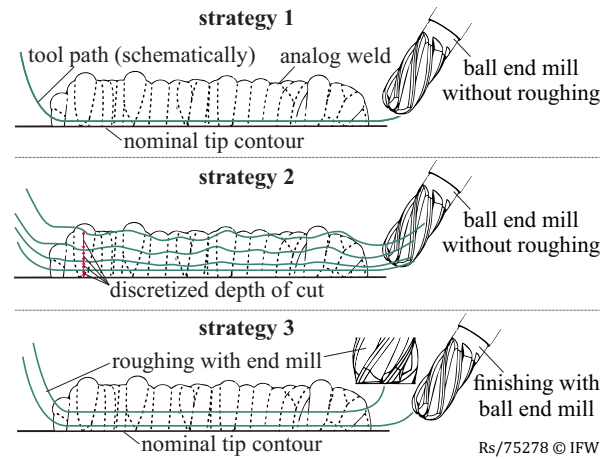


Fig. 8. Process strategies for re-contouring

By considering the shape of the weld during re-engineering of the blade measurements, the re-contouring strategies are adapted to the individual shape of the weld. This has been done for tool path strategy 2. In contrast to strategy 1, strategy 2 achieves a constant depth of cut  $a_p$  by following the contour of the weld with sequential tool paths as shown schematically in figure 8. This leads to a homogeneous material removal rate and thus more equal balance and reduced cutting forces compared to strategy 1. Re-contouring strategy 3 includes a roughing step using an end mill with high removal rate, followed by a finishing step with the ball end mill. Compared to strategy 1 the process time is slightly increased to 16 min due to the roughing step. In contrast to strategies 1 and 2, the ball end mill in strategy 3 has a cutting edge radius of  $r_B = 30 \mu\text{m}$  in order to increase the compressive residual stresses based on the results in [33]. The cutting parameters for the final surface are the same for all strategies in order to evaluate the influence of the

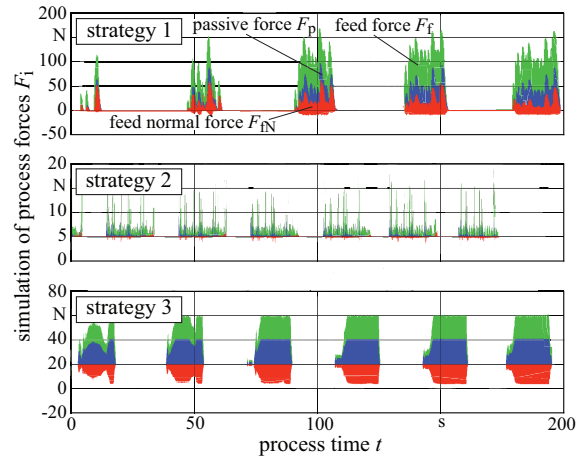
individual tool paths. All Re-contouring tool-paths have been created in the CAD/CAM-software Siemens NX 8.5. The ball end mill is inclined by using positive lead angles  $\lambda$  (draw-cut) in order to avoid the indentation effect, described in [17]. The tool path is represented by the cutter location source file (CLSF) and provides a machine independent tool-motion. The simulation is carried out with CutS, which contains necessary functions for interpreting the CLSF.

4.2. Process forces

In previous works, a 3-axis process force simulation has been validated by experiment [9]. The same method for force calculation with the consideration of 5-axis tool movement and multi-dexel workpiece model as described in section 3 is applied for all three re-contouring strategies. All three strategies were tested on the DMU 125P 5-axis milling machine tool. Due to the constantly moving machine table and resulting mass displacement of the dynamometer relative to the initial machine coordinate system, accurate force measurements are currently not reasonable. To handle this issue the process forces could be measured with sensory axis-slide [34] in the future. However, the simulation of the workpiece quality uses the simulated cutting forces. Therefore the cutting forces are validated indirectly with the results in section 4.3 and 4.4. Due to the rotating tool, a high dexel resolution is necessary for computation of the process forces. A resolution of 1024 dexel in each direction has been chosen for the weld (approx. 36 x 15 x 10 mm). Using a standard desktop computer leads to computation time of several days if the whole process is covered. Therefore, only the forces at the beginning of the re-contouring process are considered in the simulation. In addition, this has been considered sufficient for the purpose of extracting general conclusions from the different tool-path strategies. Figure 9 shows the simulated forces for the strategies 1-3 top down. For each strategy the first 5-6 tool infeeds of the ball end mill are charted. Due to the complex weld shape the ball end mill has an inconsistent depth of cut, which can be seen in strategy 1 and 2. The lowest forces appear in strategy 2 due to the constant “following”-strategy. The peaks therefore are relatively high compared to strategy 1 and 3. Using strategy 3 the ball end mill has relatively constant engagement conditions, as the weld has been roughed with an end mill before.

4.3. Surface Topography

The surface topography is mainly affected by the tool deflection and the so-called kinematic topography, which is the resulting topography by just considering the kinematics of the process and neglecting e.g. vibrations, surface deformation or chip formation. Hence the kinematic topography is mainly defined by the feed per tooth  $f_z$  and step over  $b_r$ . The tool deflection is not considered in the material removal simulation, but it can be calculated by using the simulated forces and the method described in section 3.2. This has been exemplary done at the tip of the blade for all strategies considering the transition as shown in figure 10. It is not surprising that strategy 1 leads to the highest tool deflection because of the higher cross section compared to strategy 2 and 3, whose deflections are similar to each other. However, the result in figure 10 shows a reasonable prediction of the tool deflection by simplifying the stiffness of



**simulation of process forces with ball end mill**  
 cutting speed  $v_c = 120$  m/min    depth of cut  $a_p = \text{var.}$   
 feed per tooth  $f_z = 0.20$  mm    step over  $b_r = 0.3$  mm  
 lead angle  $\lambda = \text{var.}$     tilt angle  $\tau = \text{var.}$   
 Ne/80049 © IFW

Fig. 9. Simulation data of process forces

the system machine-tool holder-tool by a cantilever beam. Furthermore the measured surface topography of strategy 1 and 3 as well as the kinematic topography is shown in figure 10 for the same area. Due to the fact that the process parameters are the same for strategy 1 and strategy 3, the simulation results in the same kinematic topography. Even though both strategies show comparable characteristics within the simulation, the measured surface of strategy 3 is more comparable to the simulation. This is due to the slightly cutting edge radius, which reduced the influence of cutting edge chipping. Another influencing factor is the appearance of vibrations for strategy 1 due to the high cross sections, which is not considered in the simulation yet. Such characteristics will be included in the future.

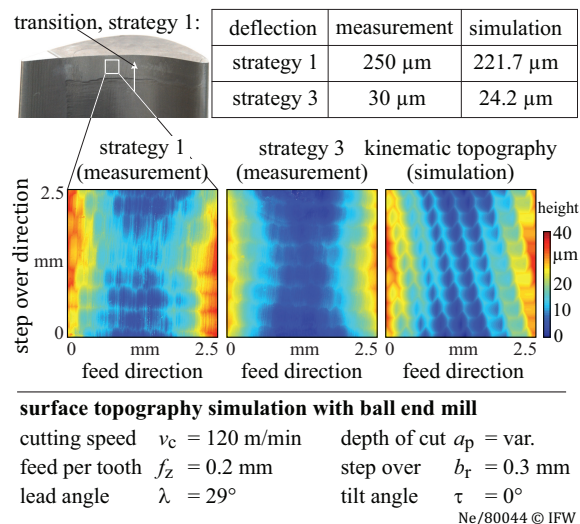


Fig. 10. Surface topography after re-contouring

#### 4.4. Residual stresses

The superficial residual stress in feed and step over direction are measured by X-ray diffractometry using a General Electric XRD 3003 TT two-circle diffractometer. All used parameters and constants for the X-ray diffraction are listed in [33]. The measurements and the parameters  $S$  divided by the empirical parameter  $K$  are shown in figure 11. It can be seen that strategy 1 and 2 lead to similar residual stresses despite different material removal rates and cross sections during re-contouring. This is due to the same micro-geometry of the cutting tool and the same surface generating forces, which is also shown by the same parameter  $S$ . The compressive residual stresses in strategy 3 are increased, even using the same cutting parameters for the ball end mill compared to strategy 1. The only difference is the roughing process with an end mill as described in section 4.1. This compressive residual stresses are increasing because of the larger cutting edge radius  $r_\beta$ . The cutting edge radius causes an increase of the surface generating ploughing forces  $F_{pl}$  while the area  $A_{sp}$  remains constant because of the constant process parameters.

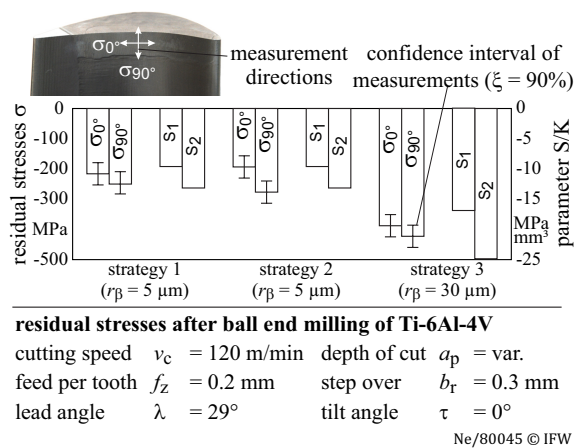


Fig. 11. Residual stress and surface generating stresses during machining

It has to be considered, that the described method is an empirical correlation between the surface generating ploughing forces  $F_{pl}$  and the area of the final generated surface  $A_{sp}$  to predict the residual stresses. However this method aims at proposing a new perception to understand the effects between surface generation and residual stresses. It has been shown that the method in [33] is also valid for 5-axis strategies, if tool indentation [17] is prevented.

#### 5. Conclusion and Outlook

The paper shows how workpiece quality of re-contouring blades evolves through different 5-axis process strategies. These strategies are

1. Ball end milling of the weld in one step
2. Follow the contour of the weld by using sequential cuts
3. Roughing with end mill and finishing with ball end milling

In this context, cutting forces, surface topography and residual stress parameters were investigated. The final surfaces of all three cases are generated with a ball end mill using the same cutting parameters, but with different tool paths. In terms of process time, strategy 1 is favourable and close to strategy 3. Following the contour is the slowest strategy and thus not yet applicable for industrial environment. Strategy 1 shows the highest tool deflection due to the high depth of cut. By using strategy 2 and 3, the tool deflection is significantly reduced due to homogenous material removal rate and thus more equal balance and reduced cutting forces.

Higher compressive residual stresses results by using cutting tools with a higher cutting edge radius, which have been done for strategy 3. Thus, strategy 3 is recommended for industrial usage. The strategy provides an increased quality of the workpiece with only a slight increase of process time compared to strategy 1. All quality results are confirmed by a simulation-based approach for the 5-axis re-contouring processes using a multi-dexel material removal simulation. It is shown that the simulation is applicable to predict certain aspects of the workpiece quality such as surface topography, residual stress or tool deflection. Simulation results fit well to the measured experimental values unless unregarded effects appear. Experimental results indicate the influence of workpiece vibration, which is not considered in the simulation, yet. Hence, the workpiece was constructed as rigid as possible. Admittedly, vibration does not occur in the finishing strategies, but re-contouring of a more realistic, thinner blade may cause vibration and deflection also in case of low depths of cut. Therefore, the prognosis of surface quality concerning tool and workpiece deflection and vibration is a main issue for further progression in this project. Furthermore, simulation time prevents to use the simulation for practical use in case of process planning. Therefore, further development of the calculation methods has to be done, to speed up the simulation, e.g. through a simplified tool model.

#### Acknowledgements

The authors thank the German Research Foundation (DFG) for the financial support within the Collaborative Research Center 871: Regeneration of complex capital goods.

#### References

- [1] Miglietti, W., Summerside, I. Repair process technology development and experience for w501f row 1 hot gas path blades. In: Proceedings of ASME Turbo Expo: Power for Land, Sea and Air. 2010.
- [2] Mohaghegh, K., Sadeghi, M.H., Abdullah, A. Reverse engineering of turbine blades based on design intent. The International Journal of Advanced Manufacturing Technology 2006;32(9-10):1009–1020.
- [3] Yilmaz, O., Gindy, N., Gao, J. A repair and overhaul methodology for aeroengine components. Robotics and Computer-Integrated Manufacturing 2010;26:190–201.
- [4] Gao, J., Chen, X., Yilmaz, O., Gindy, N. An integrated adaptive repair solution for complex aerospace components through geometry reconstruction. The International Journal of Advanced Manufacturing Technology 2008;36(11-12):1170–1179. Ball End Mill Machining of Turbine tips.
- [5] Bremer, C. Arosatec: Automated repair and overhaul system for aero turbine engine components. Tech. Rep.; BCT; Alround; ISQ; Metris; MTU; Sifco; Skytek; 2006.
- [6] Walton, P. Adaptive machining for turbine blade repair. Modern Machine Shop 2007;2(11).

- [7] Uhlmann, E., Lypovka, P. Steigerung der werkzeugstandzeit und prozesssicherheit: Bei der schweißnahtnachbearbeitung durch angepasste fräswerkzeuge. *ZWF* 2013;108(7-8):504–508.
- [8] Brecher, C., Klocke, F., Breitbach, T., Do-Khac, D., Heinen, D., Karlberger, A., et al. A hybrid machining center for enabling new die manufacturing and repair concepts. *Prod Eng Res Devel* 2011;5(4):405–413.
- [9] Böß, V., Nespör, D., Samp, A., Denkena, B.. Numerical simulation of process forces during re-contouring of welded parts considering different material properties. *CIRP Journal of Manufacturing Science and Technology* 2013;6(3):167–174.
- [10] Denkena, B., Boess, V., Nespör, D., Rust, F., Floeter, F. Approaches for improving cutting processes and machine tools in re-contouring. *Procedia [CIRP]* 2014;22(0):239 – 242. Proceedings of the 3rd International Conference in Through-life Engineering Services.
- [11] Al-Habaibeh, A., Gindy, N., Parkin, R.M.. Experimental design and investigation of pin-type reconfigurable clamping system for manufacturing aerospace components. *Journal of Engineering Manufacture* 2003;217:1771–1777.
- [12] Möhring, H.C., Flöter, F., Denkena, B.. Messtechnische Analyse formflexibler Spannmethode. *wt-online* 2012;11/12:795–800.
- [13] Markopoulos, A.P., Davim, J.P. *Finite Element Method in Machining Processes*. Springer London Heidelberg New York Dordrecht, 2013.
- [14] Oxley, P.L.B.. *The Mechanics of Machining: An Analytical Approach to Assessing Machinability*. Ellis Horwood Limited, Chichester, England; 1989.
- [15] Altintas, Y., Engin, S.. Mechanics and dynamics of general milling cutters. part i: helical end mills. *International Journal of Machine Tools & Manufacture* 2001;41:2195–2212.
- [16] Arrazola, P.J., Özel, T., Umbrello, D., Davies, M., Jawahir, I.S.. Recent advances in modelling of metal machining processes. *CIRP Annals - Manufacturing Technology* 2013;62(2):695–718.
- [17] Tuysuz, O., Altintas, Y., Feng, H.Y.. Prediction of cutting forces in three and five-axis ball-end milling with tool indentation effect. *International Journal of Machine Tools and Manufacture* 2013;66(0):66–81. URL: <http://www.sciencedirect.com/science/article/pii/S0890695512002064>. doi:10.1016/j.ijmactools.2012.12.002.
- [18] Elbestawi, M., Ismail, F., Yuen, K.. Surface topography characterization in finish milling. *International Journal of Machine Tools and Manufacture* 1994;34(2):245–255.
- [19] Liu, N., Loftus, M., Whitten, A.. Surface finish visualisation in high speed, ball nose milling applications. *International Journal of Machine Tools and Manufacture* 2005;45(10):1152–1161.
- [20] Buj-Corral, I., Vivancos-Calvet, J., Domínguez-Fernández, A.. Surface topography in ball-end milling processes as a function of feed per tooth and radial depth of cut. *International Journal of Machine Tools and Manufacture* 2012;53(0):151–159.
- [21] Zabel, A.. *Prozesssimulation in der Zerspanung - Modellierung von Dreh- und Fräsprozessen (habilitation)*. 2010.
- [22] Minoufekr, M., Glasmacher, L., Adams, O.. Macroscopic simulation of multi-axis machining processes. In: 10th International Conference on Informatics in Control, Automation and Robotics (ICINCO). 2013..
- [23] Jawahir, I., Brinksmeier, E., M'Saoubi, R., Aspinwall, D., Outeiro, J., Meyer, D., et al. Surface integrity in material removal processes: Recent advances. *CIRP Annals - Manufacturing Technology* 2011;60:603–626.
- [24] Arrazola, P., Kortabarria, A., Madariaga, A., Esnaola, J., Fernandez, E., Cappellini, C., et al. On the machining induced residual stresses in [IN718] nickel-based alloy: Experiments and predictions with finite element simulation. *Simulation Modelling Practice and Theory* 2014;41(0):87–103.
- [25] Mondelin, A., Valiorgue, F., Rech, J., Coret, M., Feulvarch, E.. Hybrid model for the prediction of residual stresses induced by 15-5ph steel turning. *International Journal of Mechanical Sciences* 2012;58(1):69–85.
- [26] Altintas, Y., Kersting, P., Biermann, D., Budak, E., Denkena, B., Lazoglu, I.. Virtual process systems for part machining operations. *CIRP Annals - Manufacturing Technology* 2014;63(2):585–605. URL: <http://dx.doi.org/10.1016/j.cirp.2014.05.007>. doi:10.1016/j.cirp.2014.05.007.
- [27] Eberlein, A.. Phases of high-tech repair implementation. In: 18th International Symposium on Airbreathing Engines (ISABE), Beijing. 2007, p. 1–8.
- [28] Denkena, B., Böß, V.. Technological nc simulation for grinding and cutting processes using cuts. In: Proceedings of the 12th CIRP Conference on Modelling of Machining Operations, Donostia-San Sebastián, Spain. 2009, p. 563–566.
- [29] Salgado, M., de Lacalle, L.L., Lamikiz, A., noa, J.M., Sánchez, J.. Evaluation of the stiffness chain on the deflection of end-mills under cutting forces. *International Journal of Machine Tools and Manufacture* 2005;45(6):727–739.
- [30] Outeiro, J., Umbrello, D., M'Saoubi, R.. Experimental and numerical modelling of the residual stresses induced in orthogonal cutting of AISI 316l steel. *International Journal of Machine Tools and Manufacture* 2006;46(14):1786–1794.
- [31] Ee, K., Jr., O.D., Jawahir, I.. Finite element modeling of residual stresses in machining induced by cutting using a tool with finite edge radius. *International Journal of Mechanical Sciences* 2005;47(10):1611 – 1628.
- [32] Guillemot, N., Winter, M., Souto-Label, A., Lartigue, C., Billardon, R.. 3d heat transfer analysis for a hybrid approach to predict residual stresses after ball-end milling. *Procedia Engineering* 2011;19:125–131. 1st CIRP Conference on Surface Integrity (CSI).
- [33] Denkena, B., Nespör, D., Böß, V., Köhler, J.. Residual stresses formation after re-contouring of welded ti-6al-4v parts by means of 5-axis ball nose end milling. *CIRP Journal of Manufacturing Science and Technology* 2014;7(4):347 – 360.
- [34] Denkena, B., Litwinski, K.M., Boujnah, H.. Process monitoring with a force sensitive axis-slide for machine tools. In: 2nd International Conference on System-integrated Intelligence (SysInt): New Challenges for Product and Production Engineering. 2014, p. 1–7.